

How to connect the over- and underdoped cuprates ?

T.M.Rice

ETH Zurich

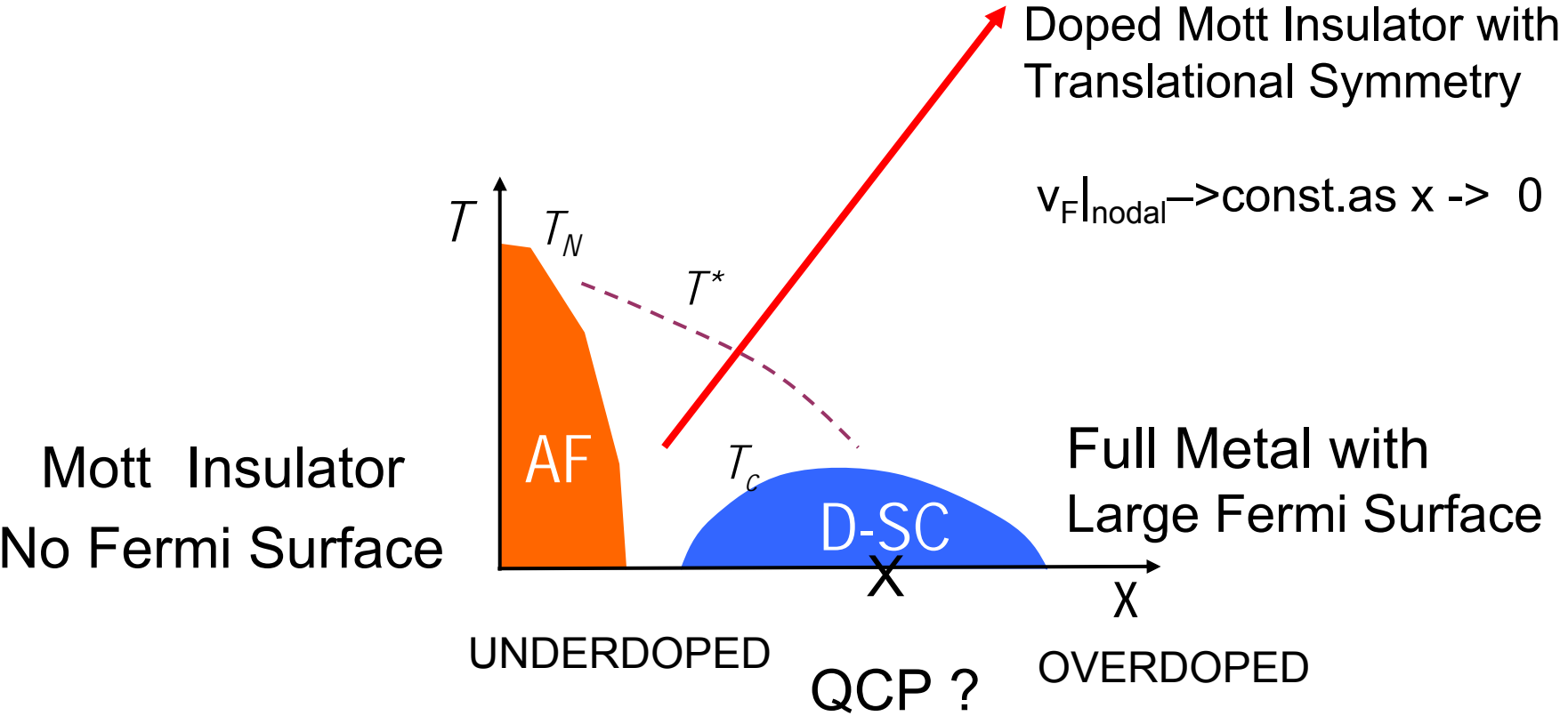
HKU & BNL

- Limits: Overdoped & Stoichiometric Undoped Cuprates are well Understood.
- Transition between them is the Challenge
 - a strong coupling Many-Body Problem
- Two Tracks: `a priori` & phenomenological theories

KITP July 2009

How do cuprates crossover from full metal to Mott insulator ?

Pseudogap Phase



Mott Insulator
No Fermi Surface

Doped Mott Insulator with
Translational Symmetry

$$v_{F|nodal} \rightarrow \text{const. as } x \rightarrow 0$$

UNDERDOPED

QCP ?

OVERDOPED

AF

D-SC

Full Metal with
Large Fermi Surface

T

T_N

T^*

T_c

x

x

Recent Experiments on Single Layer Overdoped $Tl_2Ba_2CuO_{6+x}$

using angular magnetoresistance oscillations (AMRO)

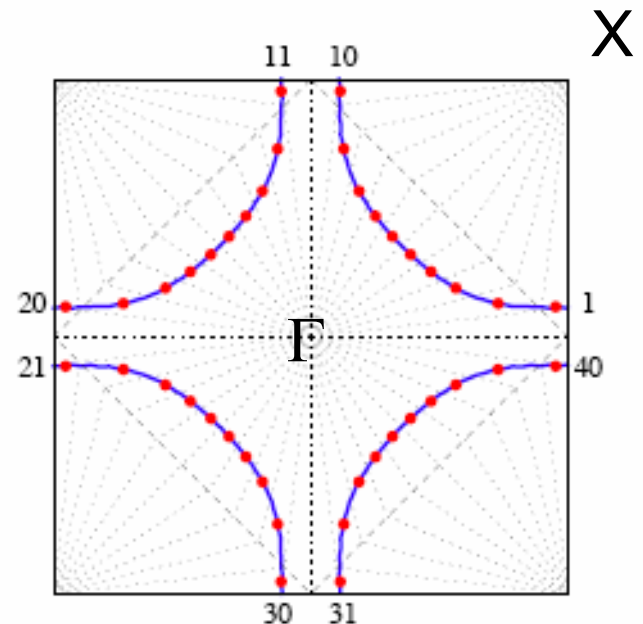
to study the anomalous transport properties in high fields

uncovered strongly anisotropic scattering around Fermi surface

which leads to the breakdown of Landau Fermi Liquid behavior :

AMRO Hussey and collaborators

Full Metallic Fermi surface
confirmed by Quantum Osc.
Vignolle et al Nature '08

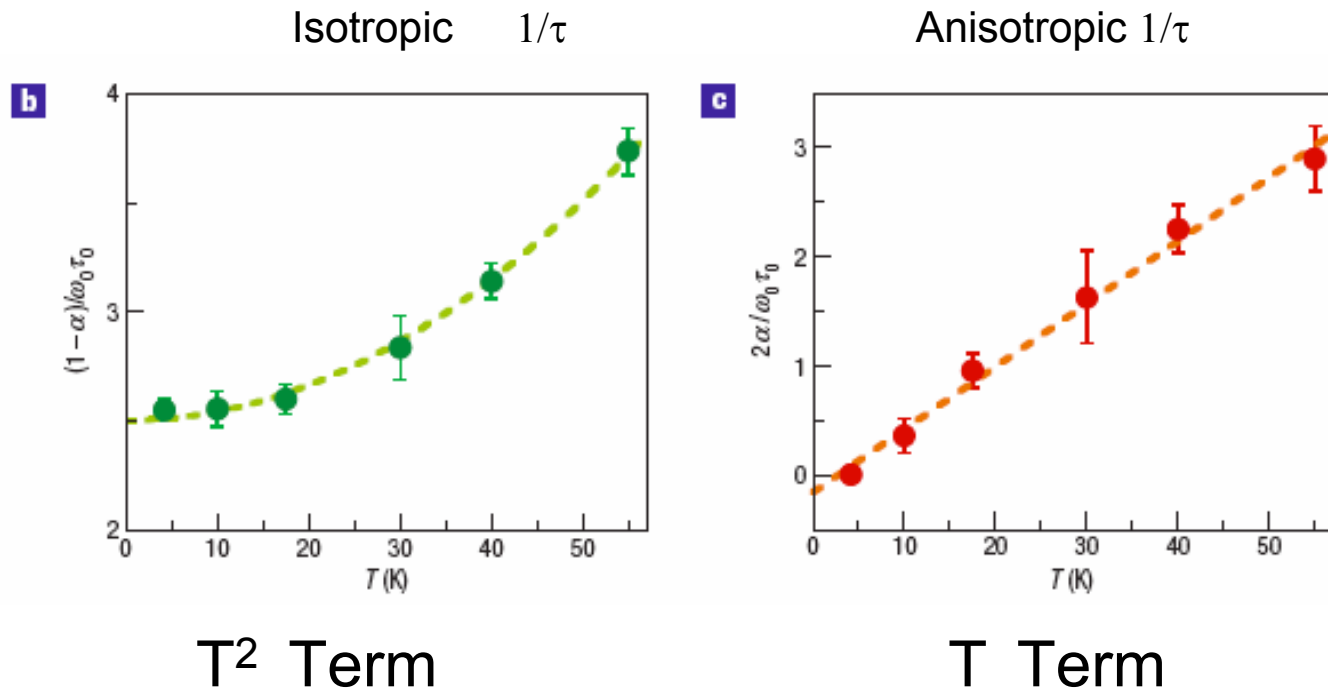


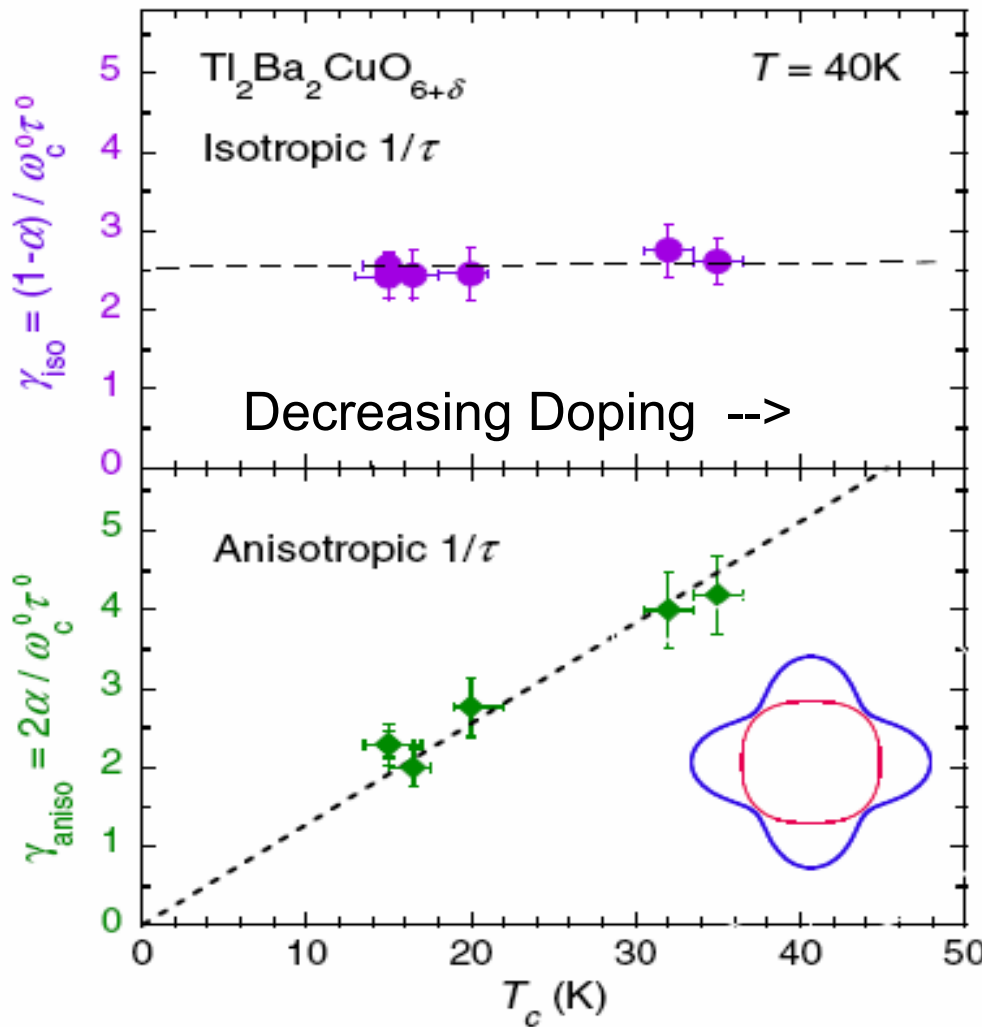
Anomalous Transport in Normal State at Onset of Superconductivity in Overdoped $Tl_2Ba_2CuO_{6+x}$

Abdel-Jawad et al. Nature Phys. 2,821`06 & PRL,99,1072`07

$1/\tau$ AMRO in High Fields $B = 45T$ determines the scattering rate around the full Fermi Surface

$1/\tau$ has **isotropic** and **anisotropic** angular components





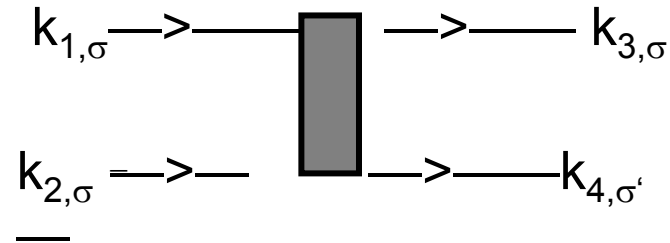
Rising anisotropic
 T-linear inelastic
 scattering appears
 at the onset of
 superconductivity
 $\approx \square \square \square \square \square$
 $\text{const}(1 + \cos(4\phi))$

Maxima at anti-nodal
 regions

FIG. 2 (color online). Top. Doping dependence of $\gamma_{\text{iso}} \equiv (1 - \alpha) / \omega_c^0 \tau^0$ at $T = 40$ K. Bottom. Doping dependence of $\gamma_{\text{aniso}} \equiv 2\alpha / \omega_c^0 \tau^0$ at $T = 40$ K and $\varphi = 0$. Here we have assumed $\beta = 0$. For $\beta = \pm 0.1$ (our range of uncertainty in β), the γ_{iso} (γ_{aniso}) points are shifted by ± 0.4 (∓ 0.4), respectively. Inset: In-plane variation of γ_{aniso} (thick blue line) with respect to $k_F(\varphi)$ (thin red line).

Use a fRG method to analyse a 1- band Hubbard Model with experimental bandstructure and moderate $U = 4t_1$

$V(\mathbf{k}_1, \mathbf{k}_2, \mathbf{k}_3)$
interaction vertex

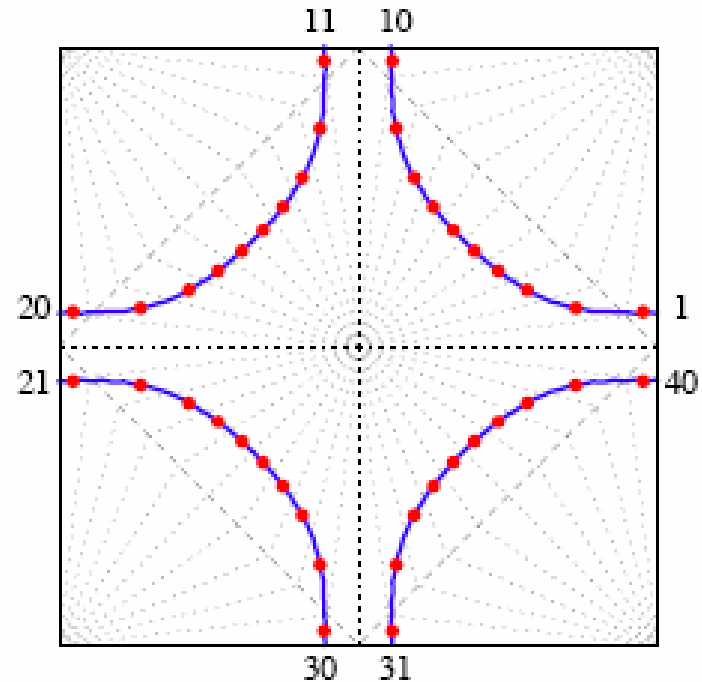


\mathbf{k}_4 determined by momentum conservation including umklapp processes

Discretize: $V(\mathbf{k}_1, \mathbf{k}_2, \mathbf{k}_3)$ constant for $\mathbf{k}_1, \mathbf{k}_2$ and \mathbf{k}_3 in same patch.

Calculate $V(\mathbf{k}_1, \mathbf{k}_2, \mathbf{k}_3)$ for $\mathbf{k}_1, \mathbf{k}_2, \mathbf{k}_3$ on Fermi surface

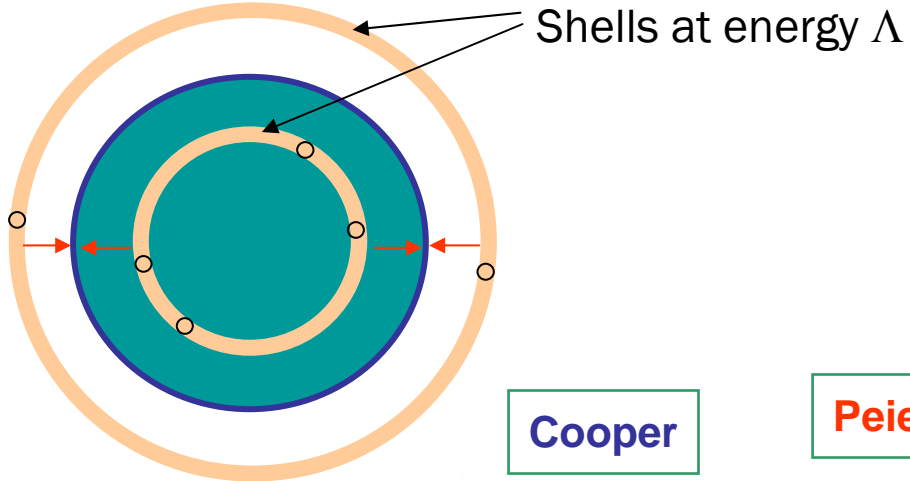
-N-patch fRG method introduced by Zanchi & Schulz '97
Also Honerkamp et al PRB '99 & - - -



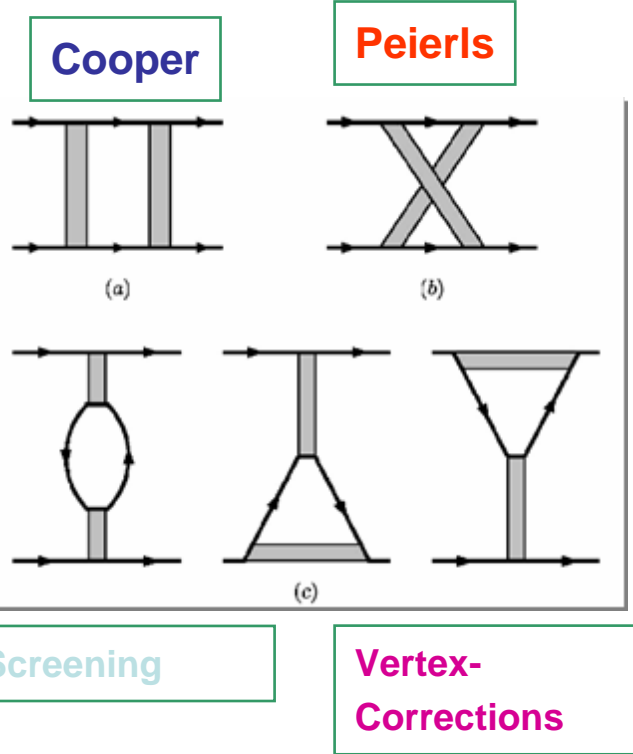
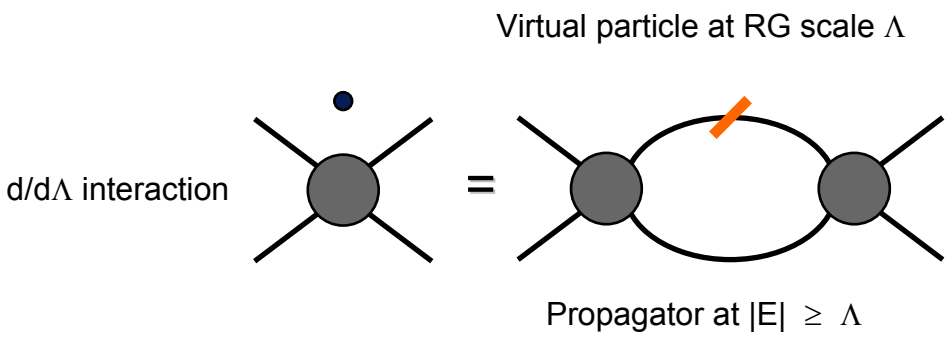
Large Fermi Surface of overdoped $\text{Ti}_2\text{Ba}_2\text{CuO}_{6+x}$ divided into 40 patches

Unbiased Approach to Interactions in a Fermi Liquid: One-Loop Renormalization Group

Strategy: Integrate out modes with decreasing energy



General structure at one loop:



$V_{\Lambda}(k_1, k_2, k_3)$ develops pronounced structure in k-space
which increases as the cutoff Λ decreases

For parameters $U=4t_1$, hole doping $x = 0.22$ & expt. bandstructure
the Cooper channel with d-wave pairing dominates the flow.

=> finite T_C for d-wave superconductivity at this density in zero field.

Expts are in finite field $B = 45\text{T}$ & $T_C = 0$ --> Too difficult for fRG !

Introduce elastic scattering $1/\tau_0$ to suppress d-wave pairing divergence at a finite scale and to mimic effect of finite field.

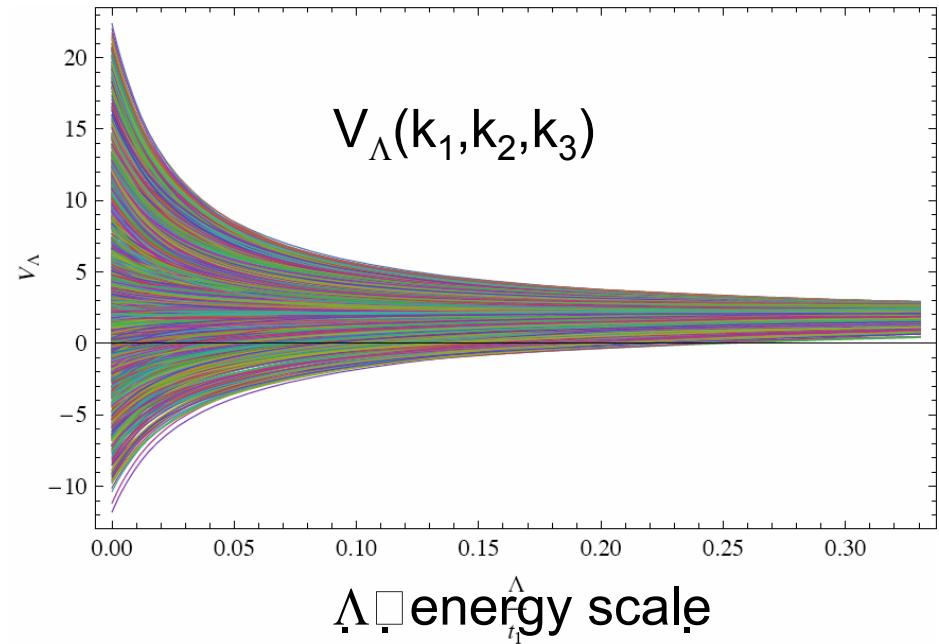
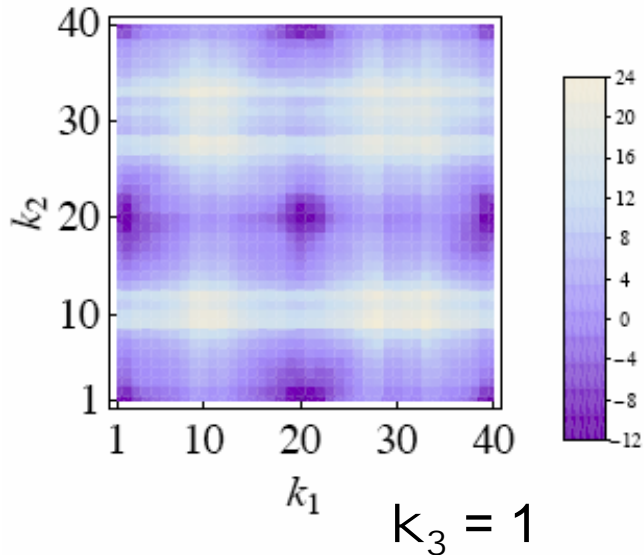
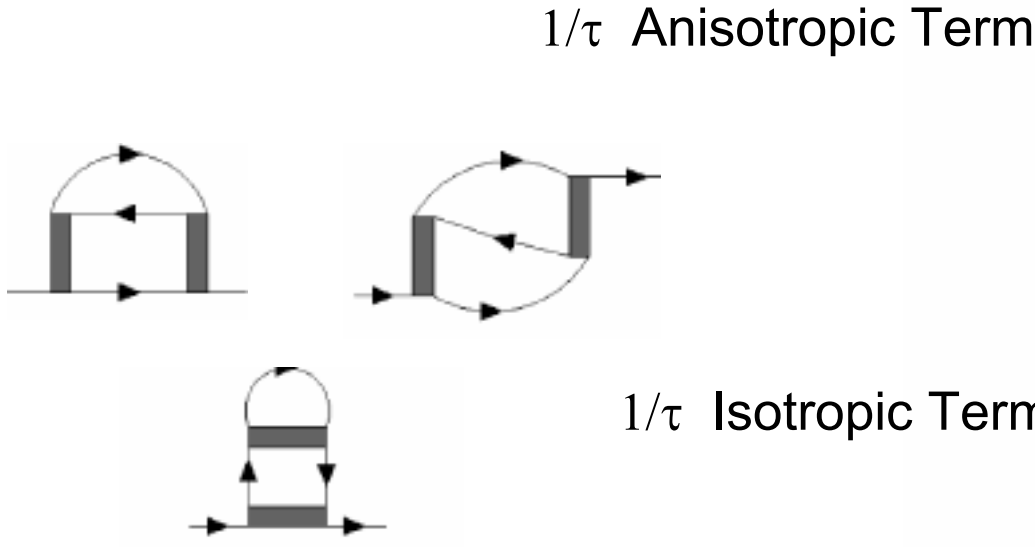


FIG. 2: (Color online) Characteristic momentum dependence of the renormalized vertex $V_\Lambda(\mathbf{k}_1, \mathbf{k}_2, \mathbf{k}_3)/t_1$ for $p = 0.22$, $T = 0.02t_1$, $1/\tau_0 = 0.2t_1$ at $\Lambda = 0$. In the figure, the dependence on the two ingoing wave vectors $(\mathbf{k}_1, \mathbf{k}_2)$ is shown, where the outgoing wave vector \mathbf{k}_3 is taken to lie in patch 1 close to $(\pi, 0)$ (cf. Fig. 1) and \mathbf{k}_4 is fixed by momentum conservation.

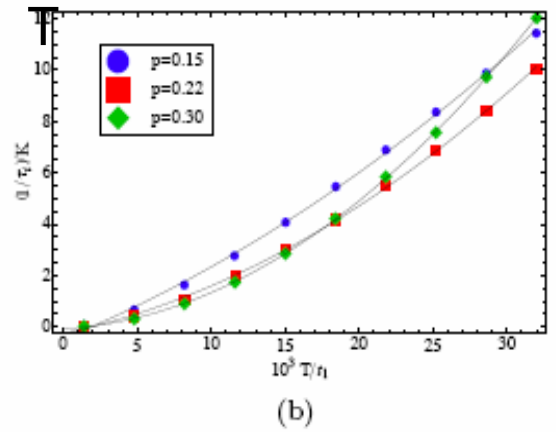
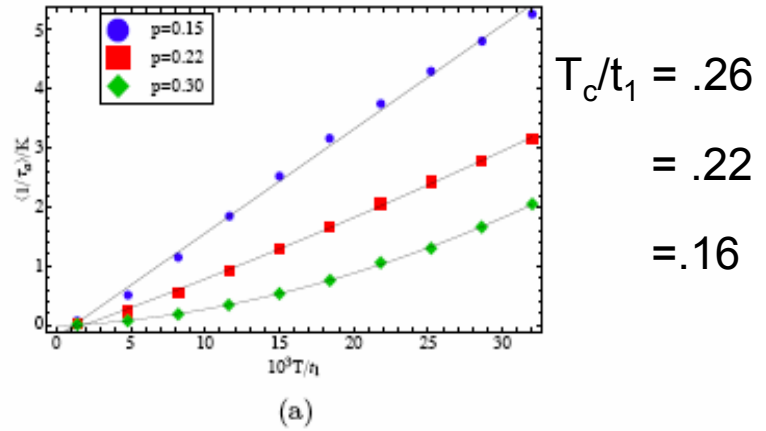
$$U=4t_1$$

$V_\Lambda(\mathbf{k}_1, \mathbf{k}_2, \mathbf{k}_3)$ continues to develop structure in p-p umklapp & p-h channels and increase as cutoff Λ decreases. No finite scale divergence however.

Results of fRG calculation



Self energy graphs



T

FIG. 5: (Color online) Temperature dependence of (a) the anisotropic and (b) the isotropic component of the quasi particle scattering rate at the Fermi surface for different values of the hole doping. The solid lines are fits to quadratic polynomials in T .

Strong anisotropic scattering including p-p umklapp processes appear near the onset of dSC => Precursor of the Mott insulating state

What happens when the doping x is reduced and the scattering vertex connecting antinodal regions increases?

fRG calculations show divergences will arise in several channels which are coupled together and mutually reinforcing.

What kind of strong coupling state without symmetry breaking is stabilized ?

An example of such a RG flow is a 2-leg Hubbard ladder at half-filling with diverging flows in p-h & p-p (d-wave Cooper & umklapp)

⇒ Groundstate known from Bosonization is fully gapped insulator with strictly short range order in both AF and d-wave Cooper pairing.

⇒ Will similar behavior appear near the antinodal regions with a fully gapped region appearing near anti-nodal regions. ⇒ novel QCP ?

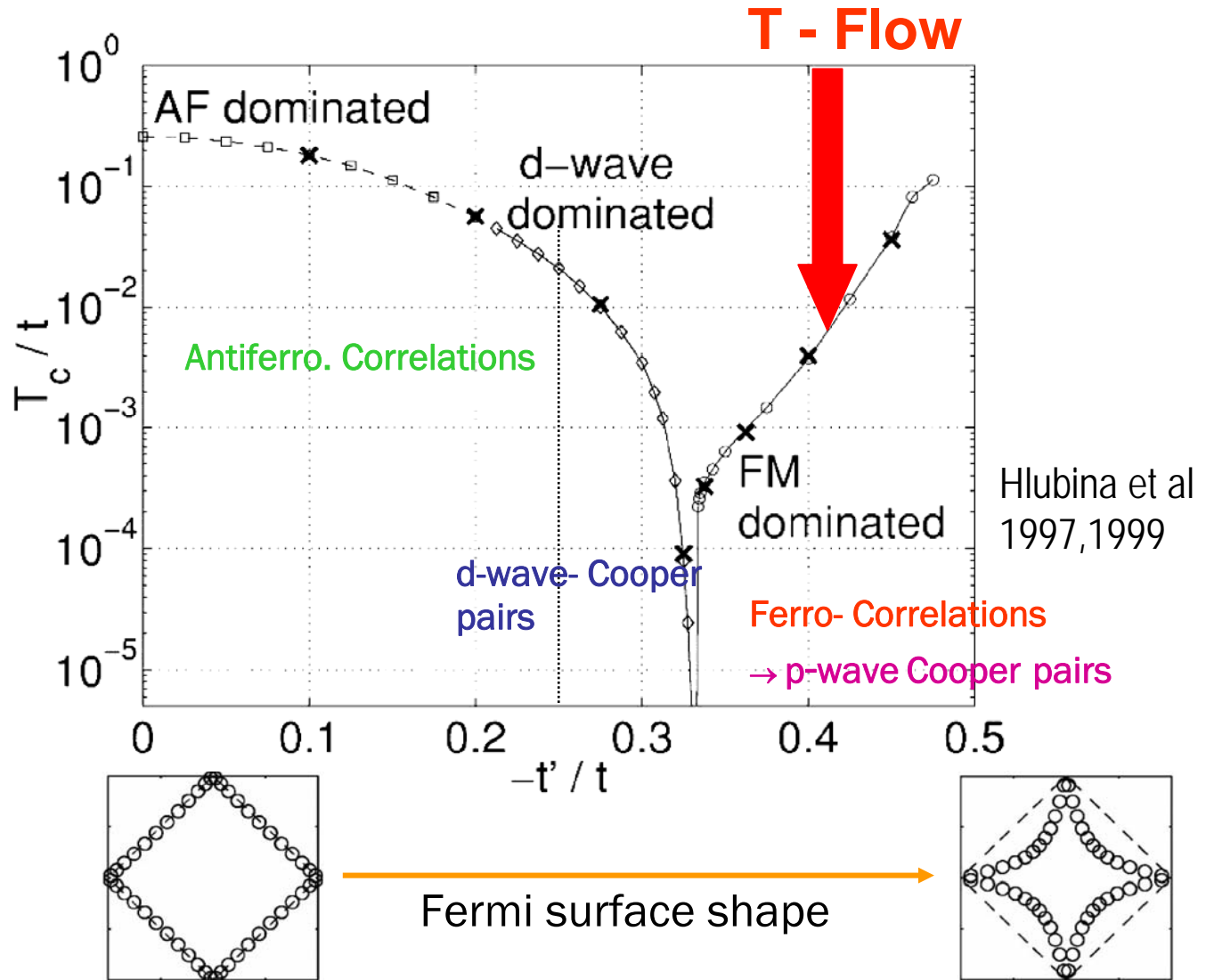
RG - Flow: from AF to FM

Honerkamp&Salmhofer 2001
C.H.,TMR & M.S. 2002

characteristic
temperature
for instability

$$U=3t$$

μ at van Hove energy



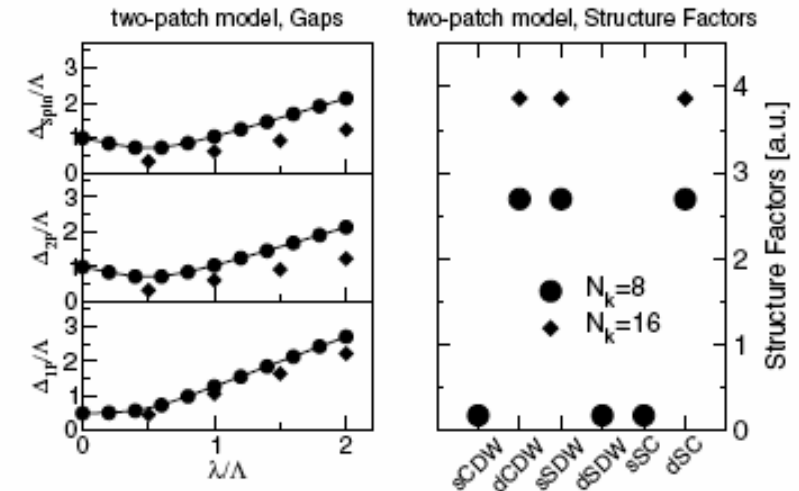
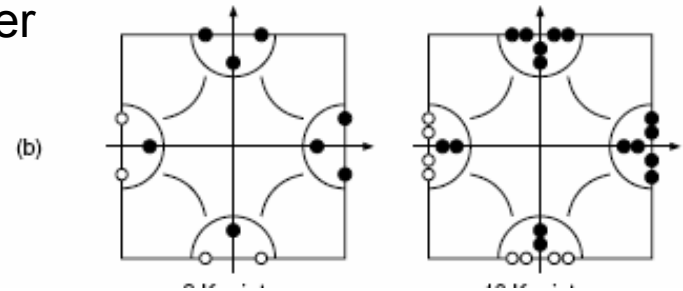
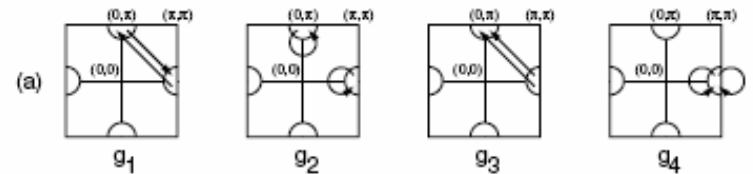
Nature of Strong Coupling State at Antinodes

d-Mott Phases in One and Two Dimensions

A. Läuchli,^{1,2} C. Honerkamp,^{2,3} and T. M. Rice²
PRL '04

Diagonalize H_{red} keeping only largest $V_{\Lambda}(k_1, k_2, k_3)$ in 1-loop RG flow
e.g. BCS diagonalized H_{red} in Cooper channel

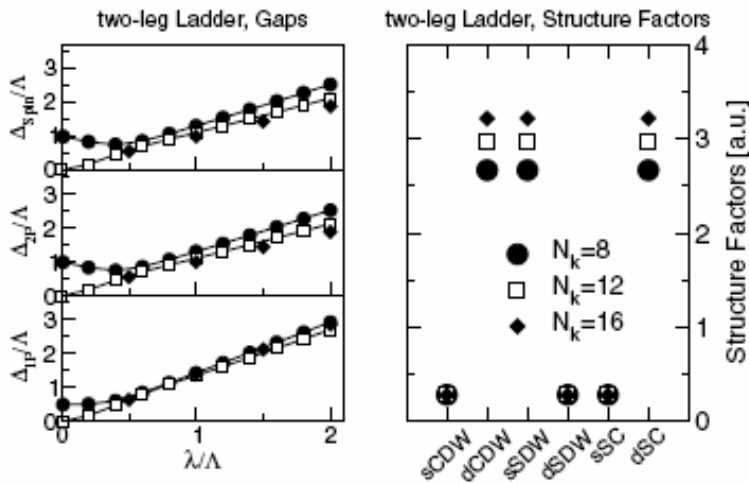
2D - Strongly Coupled Antinodal Regions



↔
similar

1D Control System 1/2 filled 2-Leg Hubbard Ladder

→ D-Mott Ins. with Charge & Spin Gaps



N_k : Number of k - points in Lanczos Algorithm

Ansatz for the Green's Fn. in analogy with 2D-coupled ladders

- K.-Y. Yang, Rice & F.C.Zhang PRB '06 see Konik, Rice & Tsvetlik PRL '05
 Berthod, Giamarchi, Biermann & Georges PRL '06

-> Gap $\Delta_R(\mathbf{k})$ opens on p-p Umklapp Surface (= AF Brillouin Zone in 2D)
 -> fixed line of zeros in $G^{RVB}(\mathbf{k}, 0)$ on Umklapp Surface

$$G^{RVB}(\mathbf{k}, \omega) = \frac{g_t}{\omega - \xi(\mathbf{k}) - \Delta_R^2 / (\omega + \xi_0(\mathbf{k}))} + G_{inc}$$

$$g_t = \frac{2x}{1+x}, g_s = \frac{4}{(1+x)^2} \quad \text{Gutzwiller Factors}$$

$$\xi_0(\mathbf{k}) = -2t(x)(\cos k_x + \cos k_y)$$

$$\Delta_R(\mathbf{k}) = \Delta_0(x)(\cos k_x - \cos k_y)$$

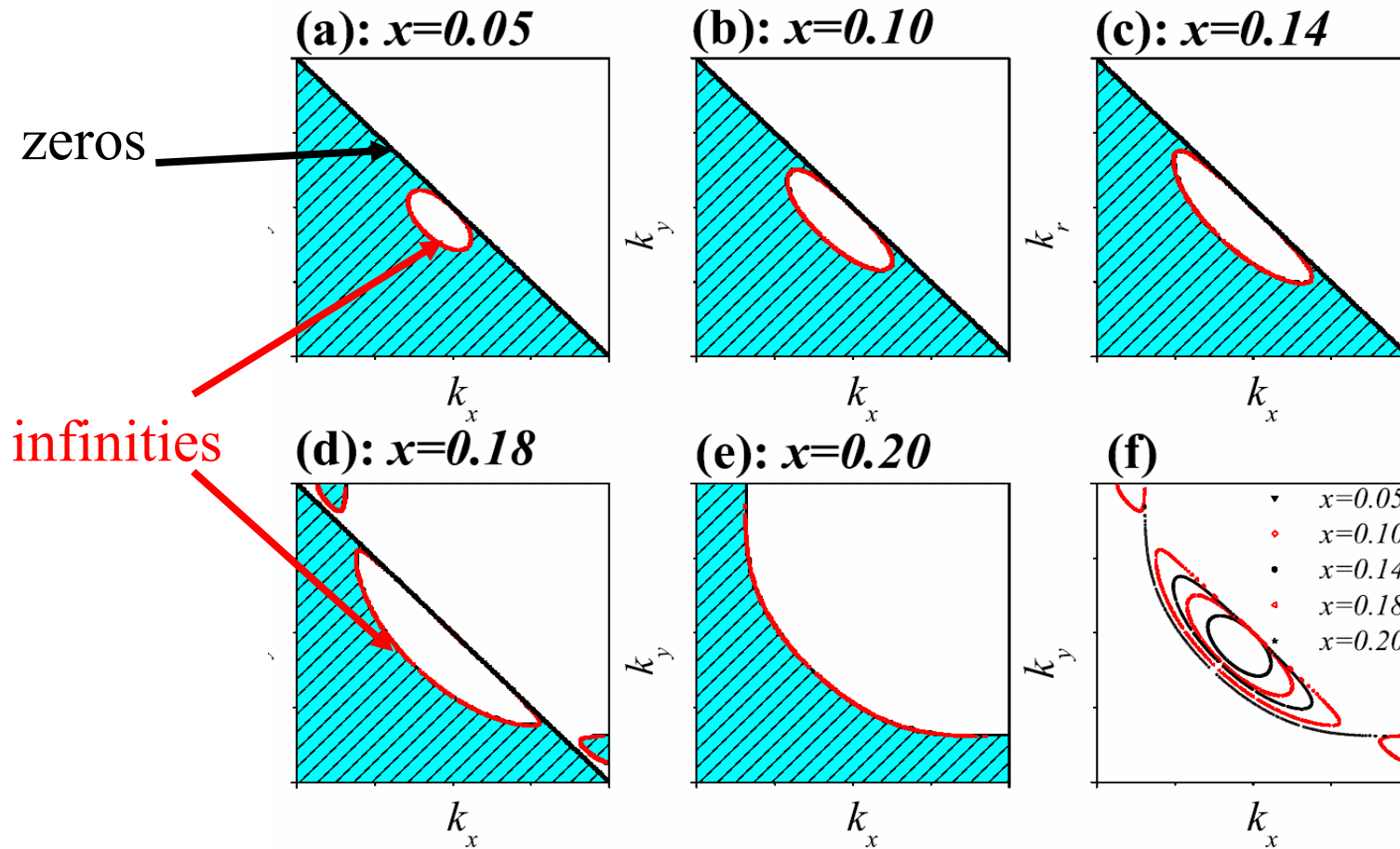
$$\xi(\mathbf{k}) = -2t(x)(\cos k_x + \cos k_y) - 4t'(x) \cos k_x \cos k_y - 2t''(x)(\cos 2k_x + \cos 2k_y) - \mu_p$$

nn	nnn	nnnn hopping
$t(x) = g_t(x)t_0 + (3/8)g_s(x)J\chi$	$t'(x) = g_t(x)t'_0$	same

$\Delta_0(x) \rightarrow 0$ at $x = x_c (= 0.2)$:
 RVB Gap from Ren. Mean Field Theory for t-J model
 - F.C. Zhang et al '88

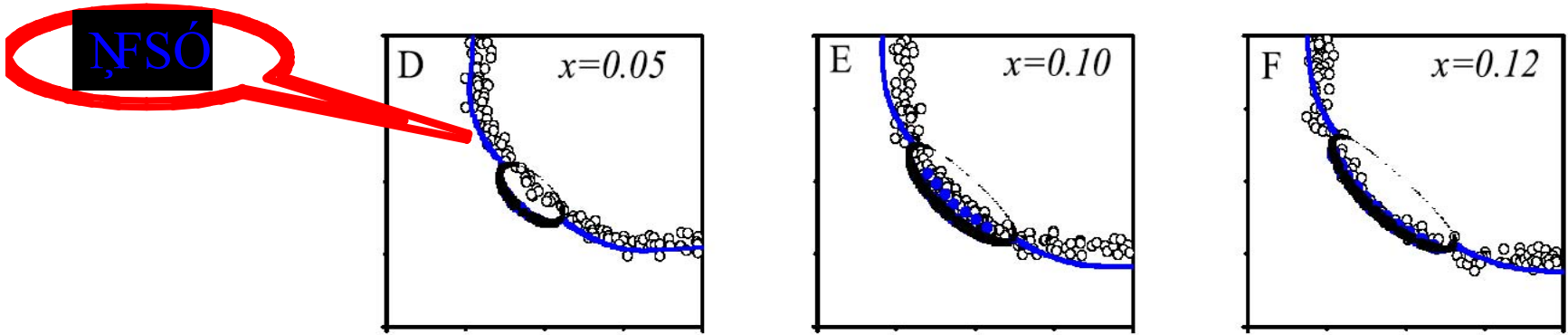
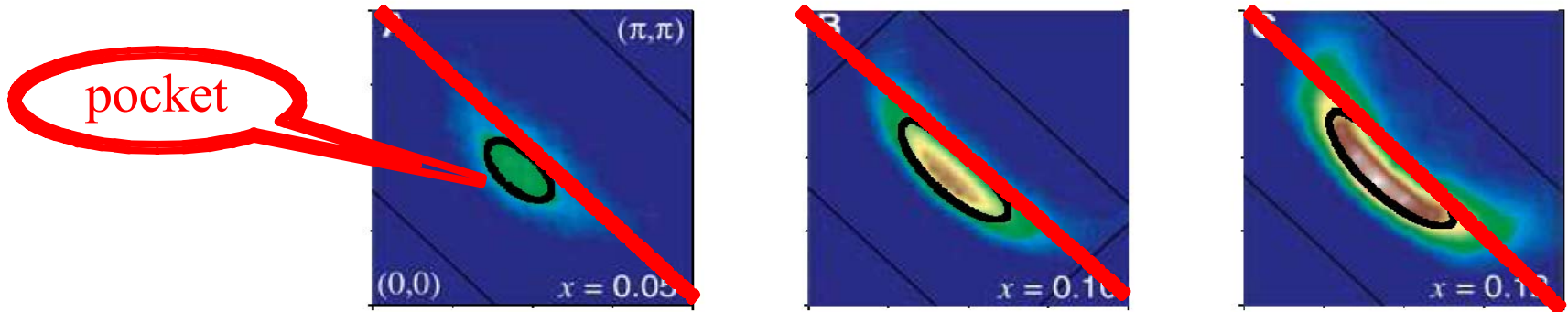
$G(\mathbf{k},0) > 0$ in shaded area bounded by zeros and infinities

Luttinger Sum Rule \Rightarrow Lines of zeros enclose 1 el./ site



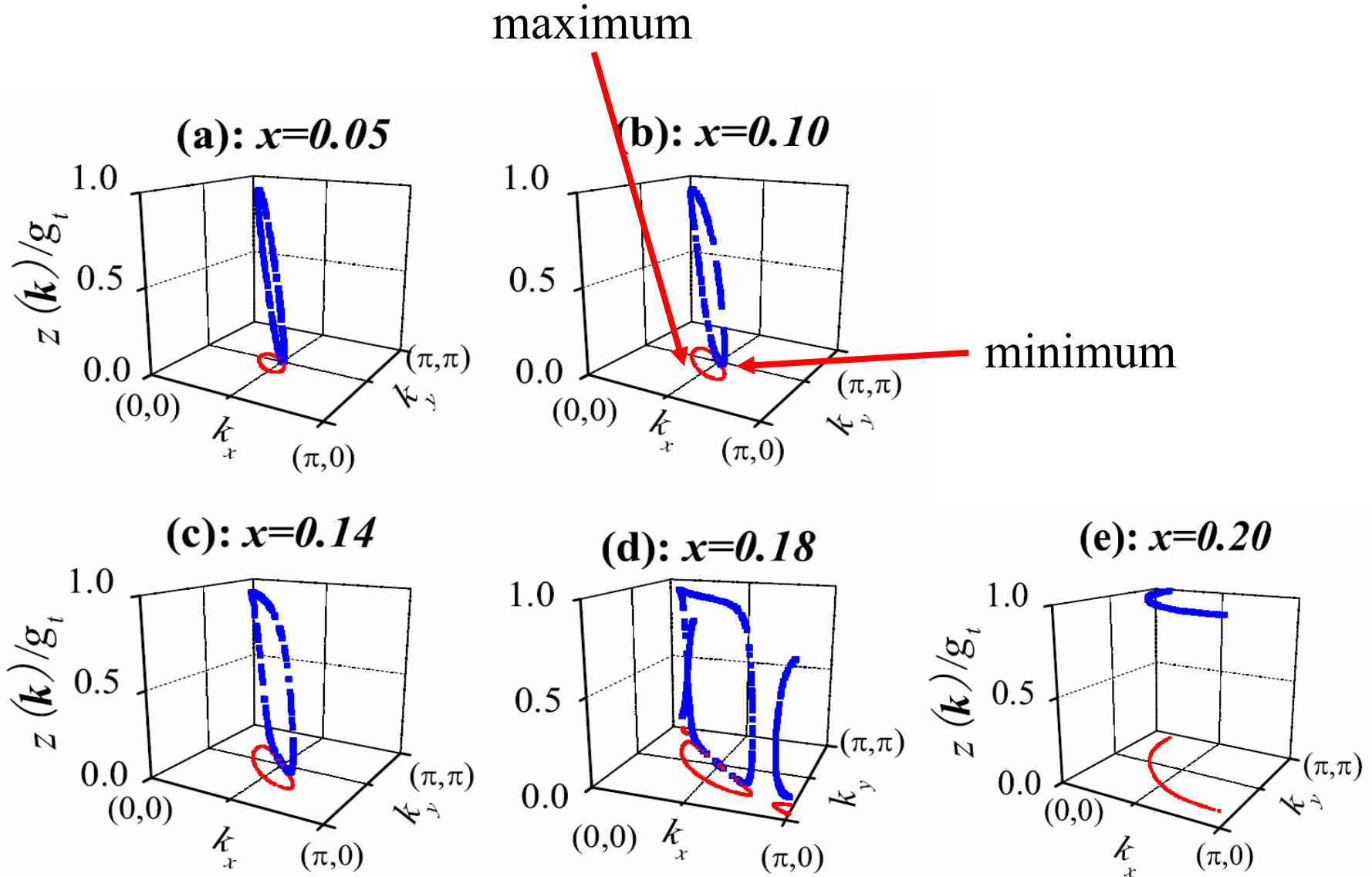
Compare Ansatz with ARPES & STM experiments on quasiparticle dispersion in underdoped cuprates

Comparison with ARPES experiments

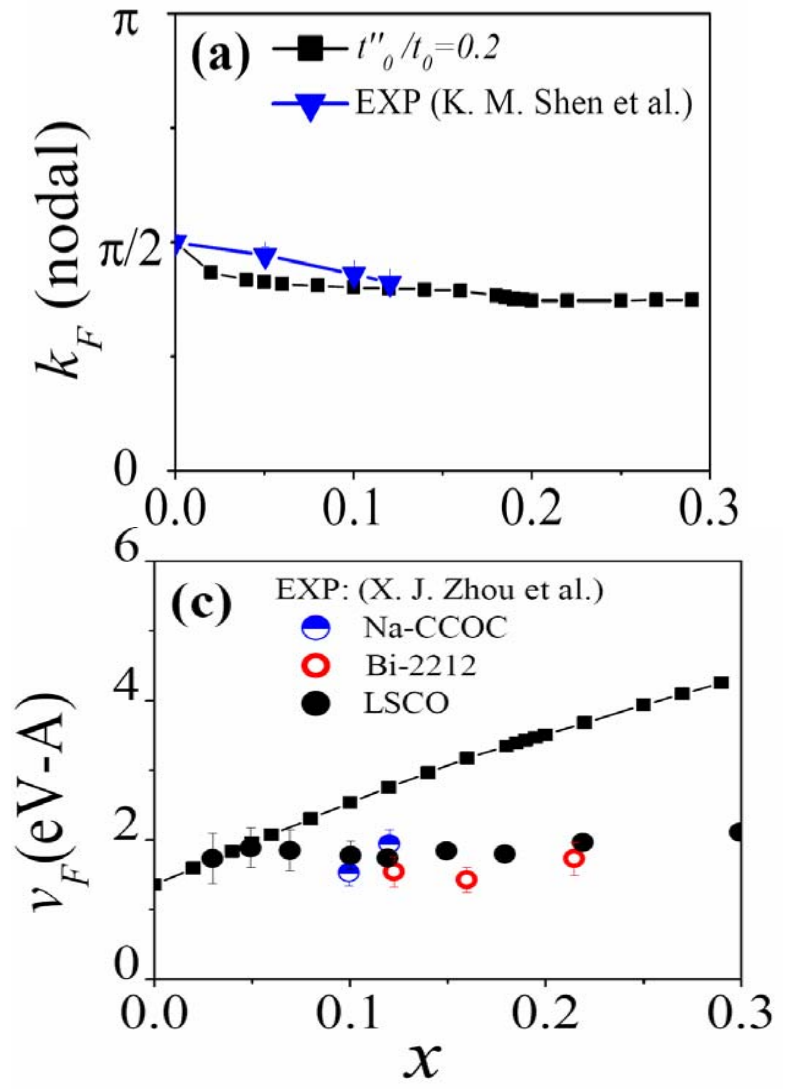
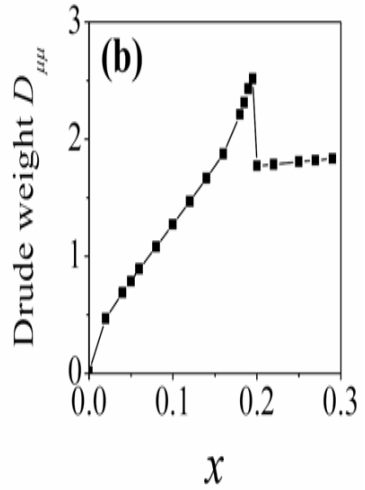
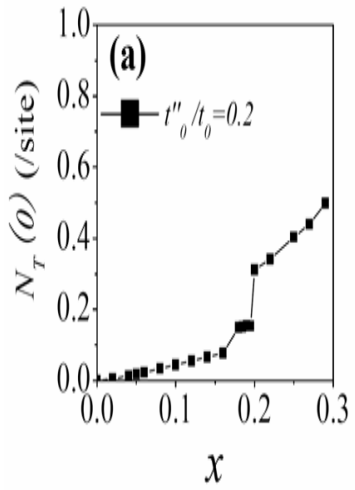
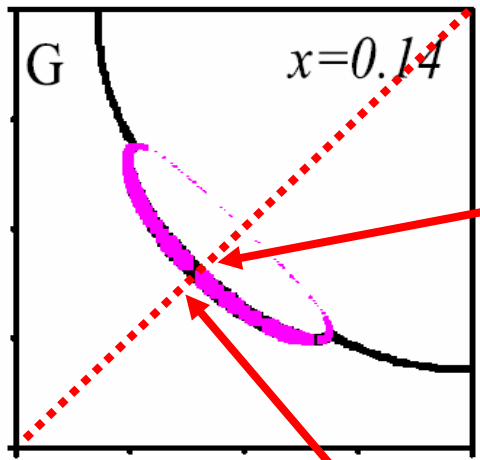


K. M. Shen et al.,
Science 307, 901
(2005)

Spectral Weight of the Coherent Quasiparticle in Pocket



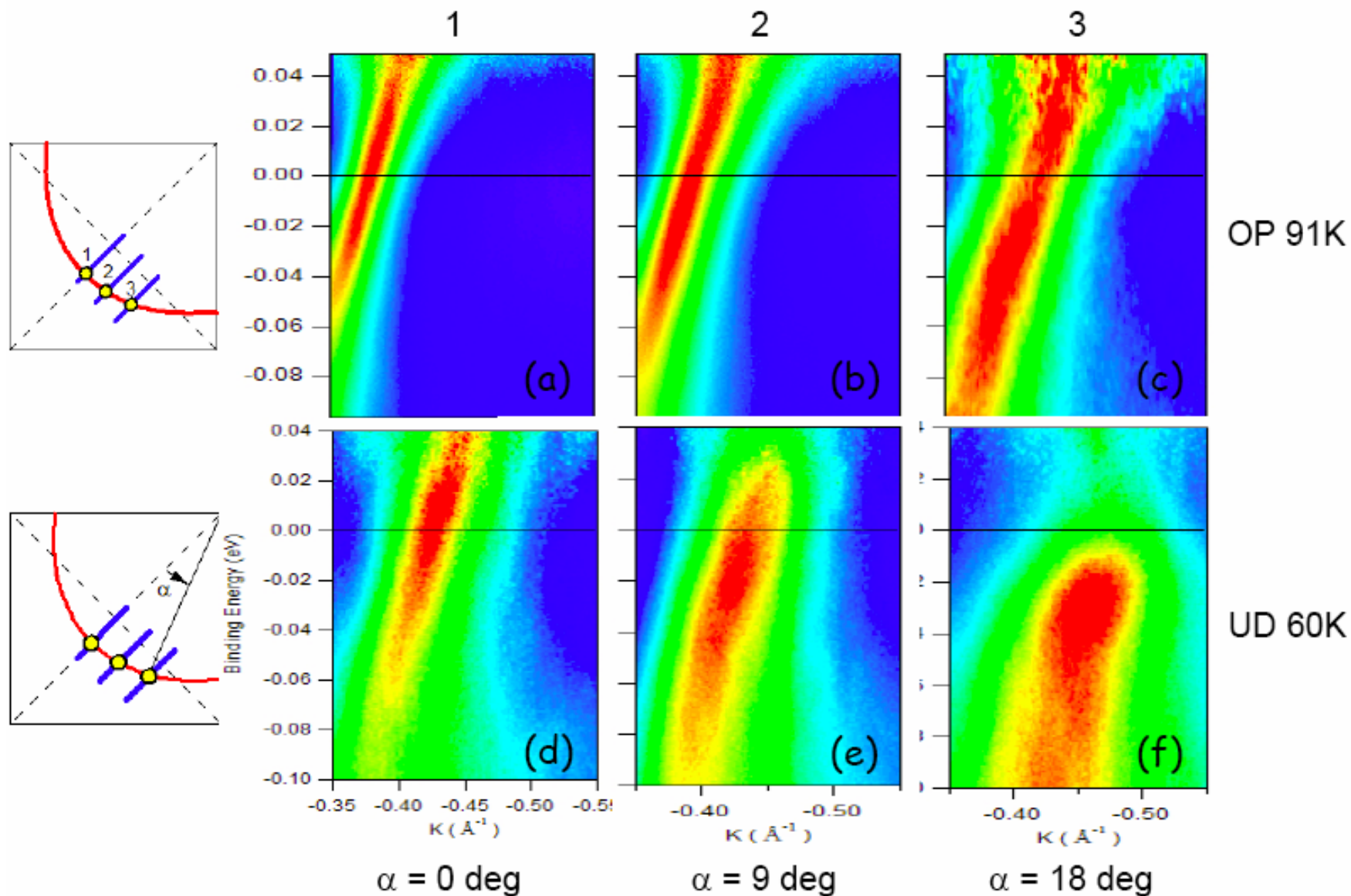
Key Parameters compared to ARPES



Particle - Hole Asymmetry in ARPES

H.B. Yang et al Nature '08

Normal state $T = 140$ K



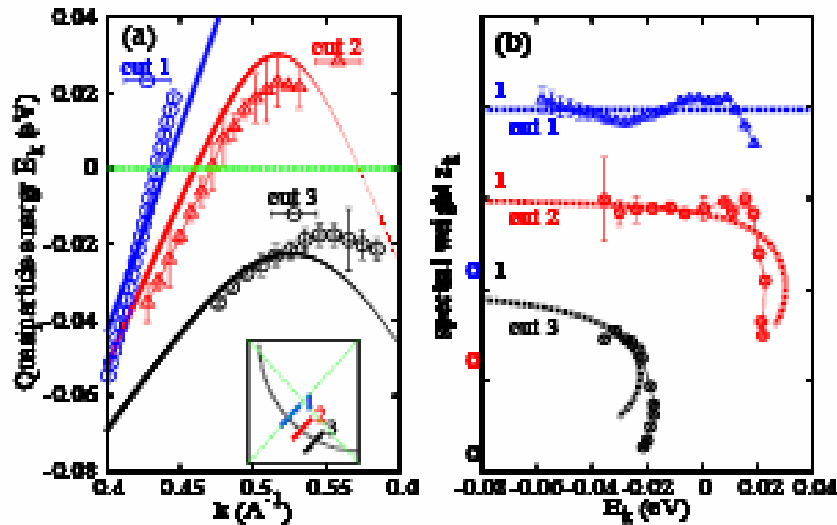


Fig. 1: (Color online) Comparisons between (a) QP dispersion E_k , (b) spectral weight z_k , from the YRZ propagator and the values obtained from the ARPES results by Yang *et al.* [1]. Error bars reflect the uncertainties in the fitting procedures; z_k at low energies in cuts 2, 3 have large error bars due to uncertainties in the choice of the rising background.

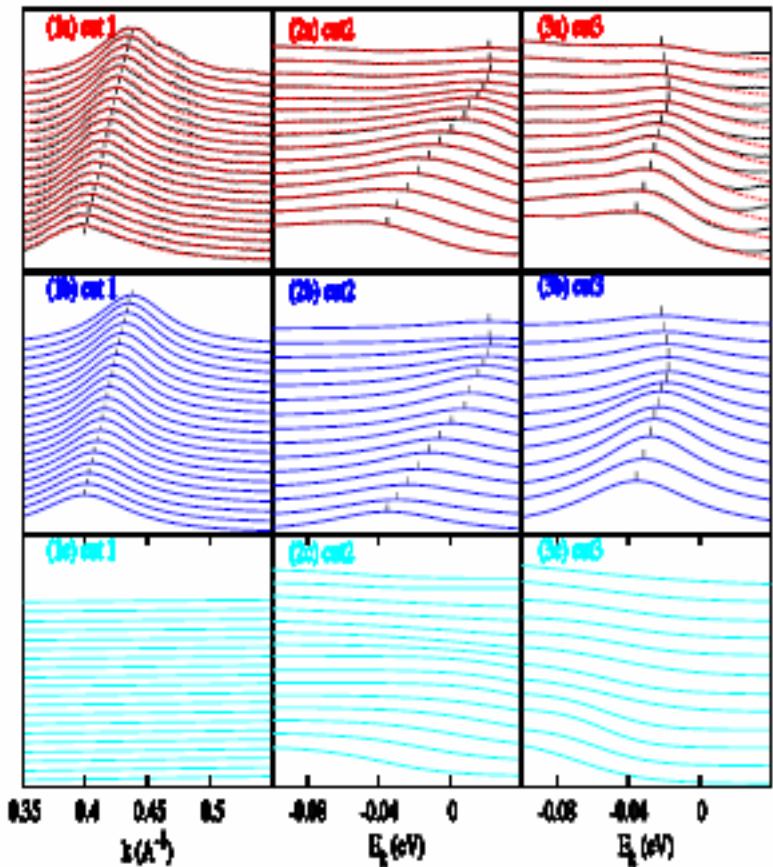


Fig. 2: (Color online) Fits to the ARPES spectra along the cuts (1-3) (see inset of Fig.1) [1]. In (1a) the MDC of cuts 1 and in (2/3a) the EDC of cuts 2 and 3 are shown, the experimental data are the solid black lines, and the fitted $A(k, \omega)$ are the dashed red lines. Individual components of the fits are displayed in (b) for QP Lorentzian peaks and (c) for smooth background $A^B(k, \omega)$.

Comparison of ARPES with YRZ ansatz

K.-Y. Yang et al EPL '09

Direct Observation of Fermi Pockets in ARPES with VUV Laser

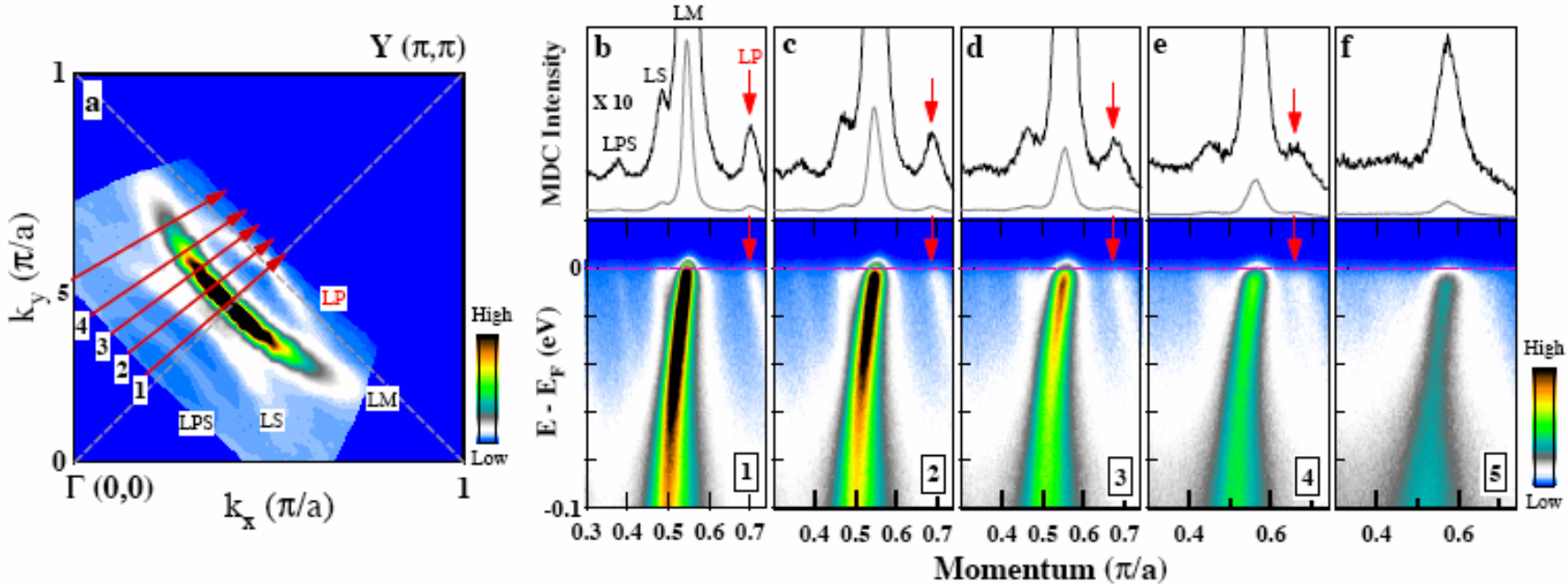


FIG. 1: Fermi surface and band structure of the La-Bi2201 UD18K sample (underdoped, $x=0.73$, $T_c=18$ K) measured at a temperature of 14 K. (a). Photoemission intensity integrated over $[-5\text{meV}, 5\text{meV}]$ energy window with respect to the Fermi level as a function of k_x and k_y . Four Fermi surface sheets are resolved in the covered momentum space, marked as LM for the main sheet, LP for Fermi pocket

Evidence for a Pocket in AIPES(Angle Integrated) - Hashimoto et al PRB 09

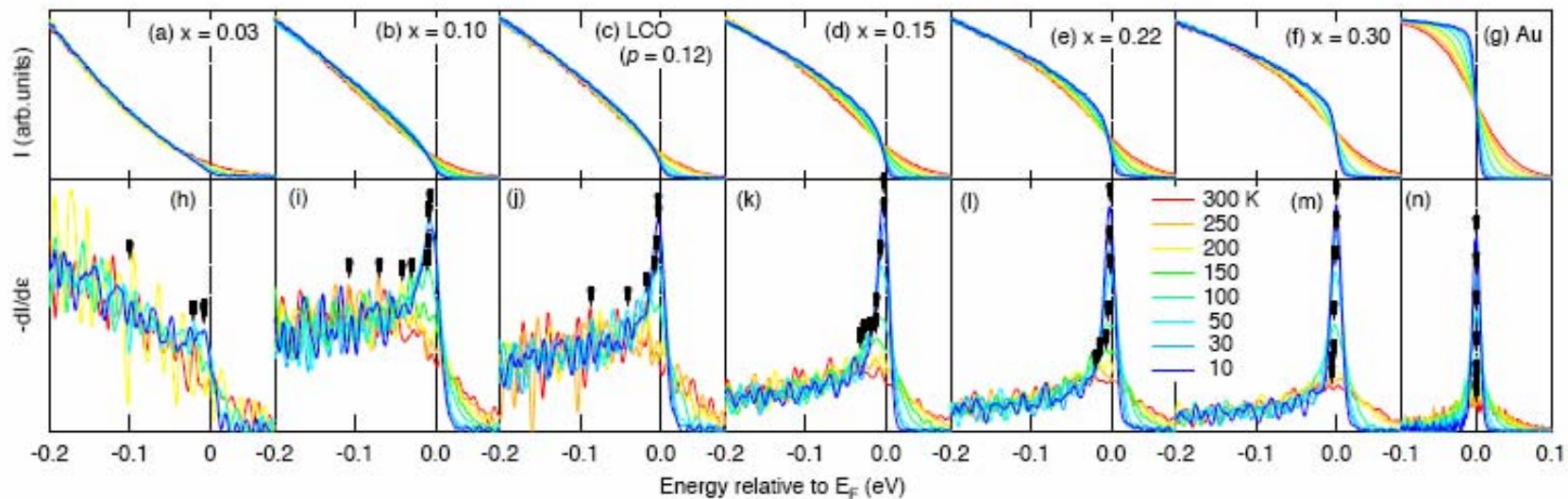
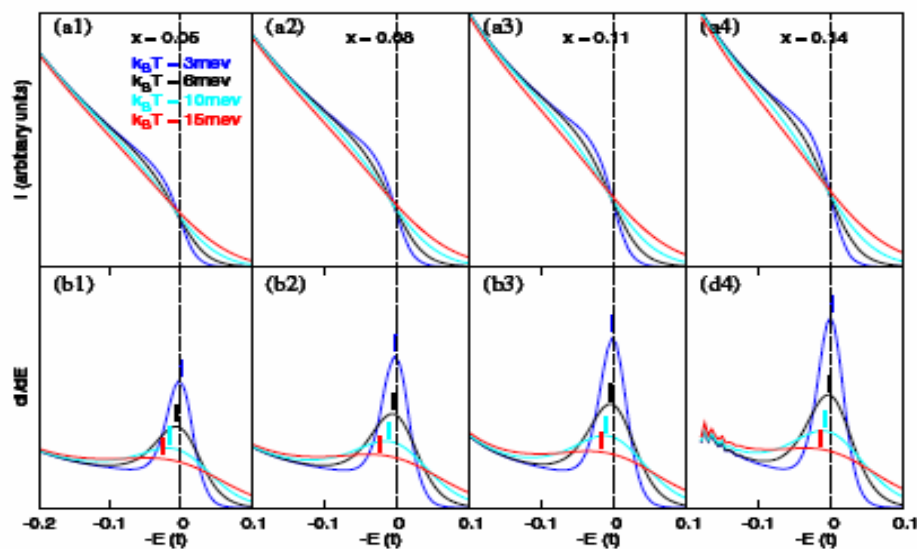


FIG. 1: (Color online) Doping and temperature dependences of the AIPES spectra near E_F for $\text{La}_{2-x}\text{Sr}_x\text{CuO}_4$ (LSCO), $\text{La}_2\text{CuO}_{4.10}$ (LCO, $p \sim 0.12$) and gold reference. (a)-(g) Raw spectra reproduced from [15]. (h)-(n) First derivative curves of the AIPES spectra. Black symbols show the peak positions.



Results using YRZ Propagator

K-Y Yang et al EPL 09

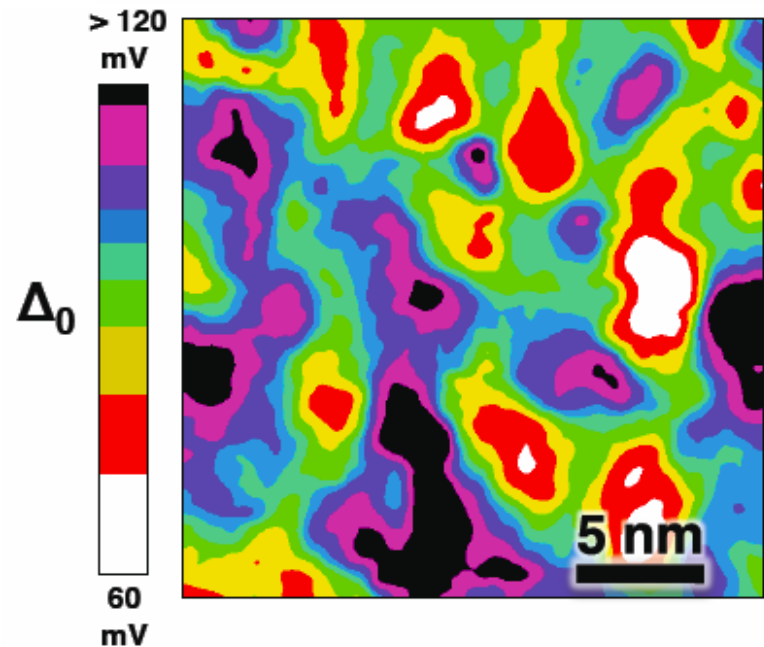
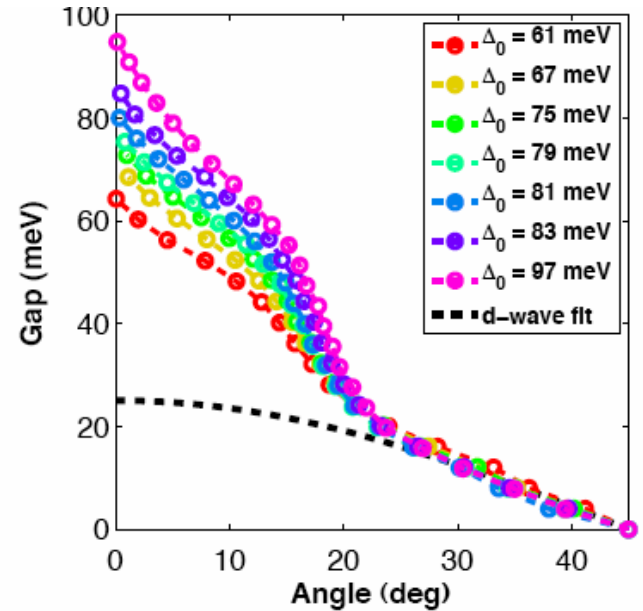
STM on underdoped BSCCO

Pushp et al Science '09

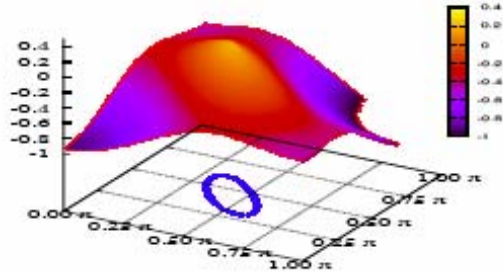
2- Gap scenario

SC gap on Fermi Arc
almost constant in a map

but antinodal gap varies strongly
in the map on 5 nm length scale



Simplest Thomas-Fermi Approx. to describe a random electric field $\phi(\mathbf{r})$



Chemical Potential of holes is a constant but Fermi energy of hole pocket varies leading to a local density $x(\mathbf{r})$ and a local breathing of Fermi arc.

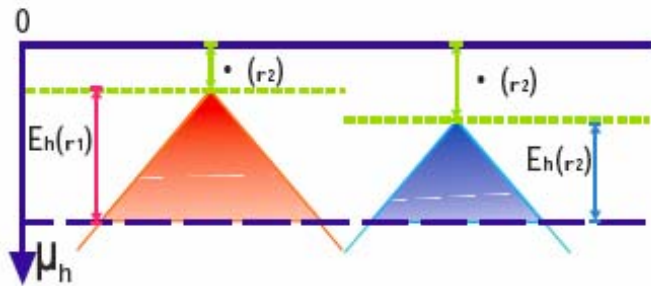
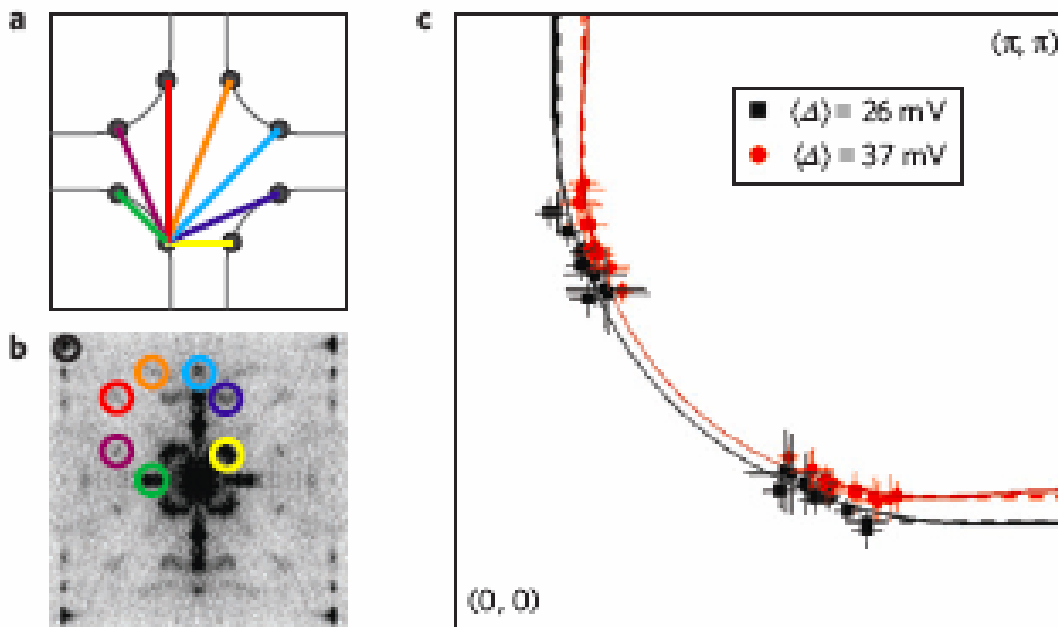


FIG. 2: (Color online) Top Panel: the low band from the single particle propagator Eq.2 in pseudogap state with the Fermi surface (hole pocket) projected on the xy plane. The bottom of the hole Fermi sea is located at the midway between the node and $(\pi/2, \pi/2)$. Lower panel: schematic demonstration of the spatial variation of the hole Fermi energy $E_h(\mathbf{r})$ due to the random electric field $\phi(\mathbf{r})$.

RVB gap $\Delta_0(x)$ varies strongly with $x(\mathbf{r})$

$\Delta_0(x) \rightarrow 0$ at $x = x_c (= 0.2)$:

RVB Gap from RMFT -Zhang et al '88

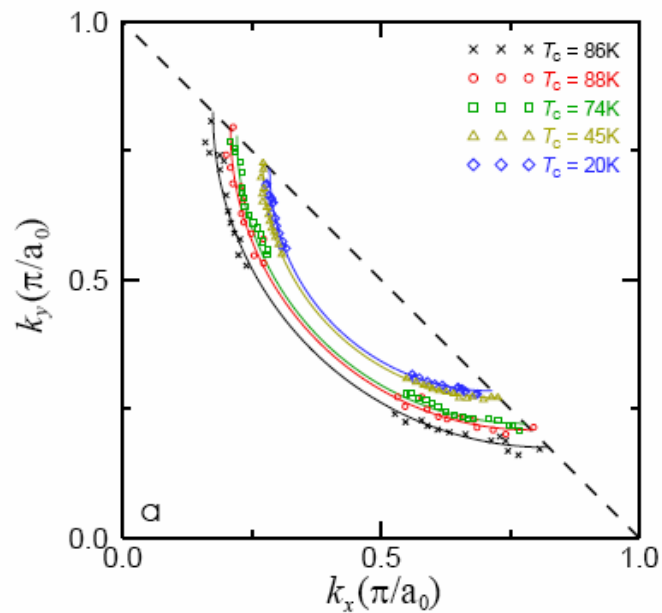


Wise et al
Nature Phys '09

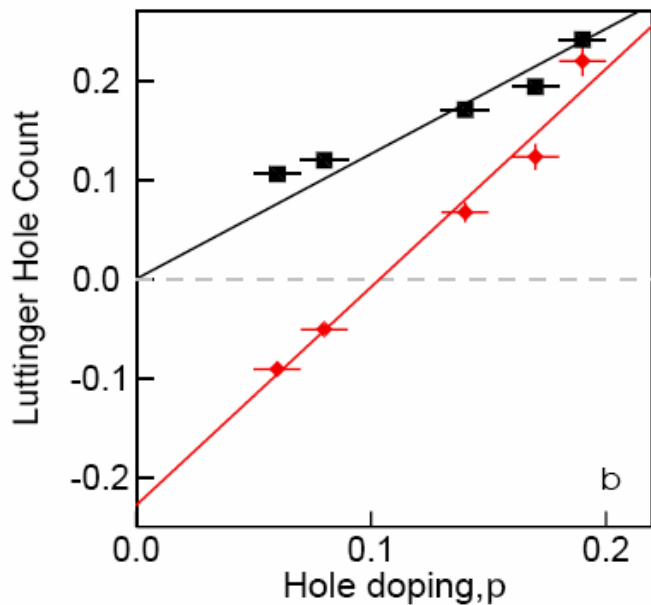
Fermi Arc breathing
locally observed
through QPI

Figure 4 | QPI-derived local FS in Bi-2212. **a**, A schematic diagram of the FS (solid line) in the first Brillouin zone, showing symmetry, leading to an eightfold replication of any points at which the density of states peaks (for example circles). Scattering between quasiparticles at these points leads to a set of interference wavevectors (coloured lines), corresponding to peaks in interference maps such as **b**, a Fourier transform of a 600 \AA , 400 pixel , $E = 12 \text{ mV}$ conductance map of 89 K overdoped Bi-2212. The positions of these peaks (defined in terms of the atomic wavevector circled in black) uniquely define a position in \mathbf{k} -space on the FS. Fitting interference peaks in a series of fast Fourier transform maps at various energies from two different masks of the same data leads to **c**, two different 'local FSs' (solid symbols with error bars indicating standard deviation for values obtained from different interference peaks). Dashed lines, obtained from checkerboard-determined nesting wavevectors, extend the determined FS to the antinode. Solid lines are FSs from a rigid-band, tight-binding model¹⁷ at two different dopings, $p = 0.10$ and 0.18 .

Coherent Quasiparticle Dispersion by STM



Kohsaka et al Nature '08



Area Enclosed by Fermi Pocket

vs.

Area Enclosed by Bandstructure Interpolation

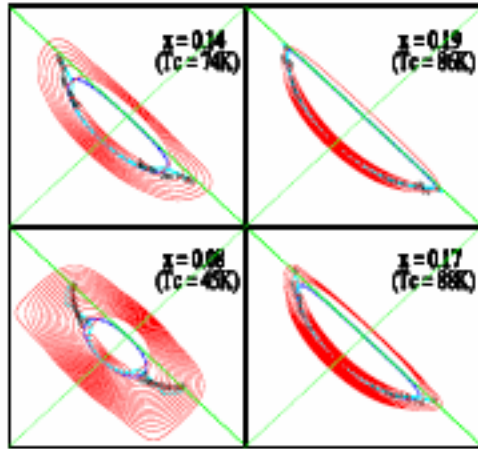
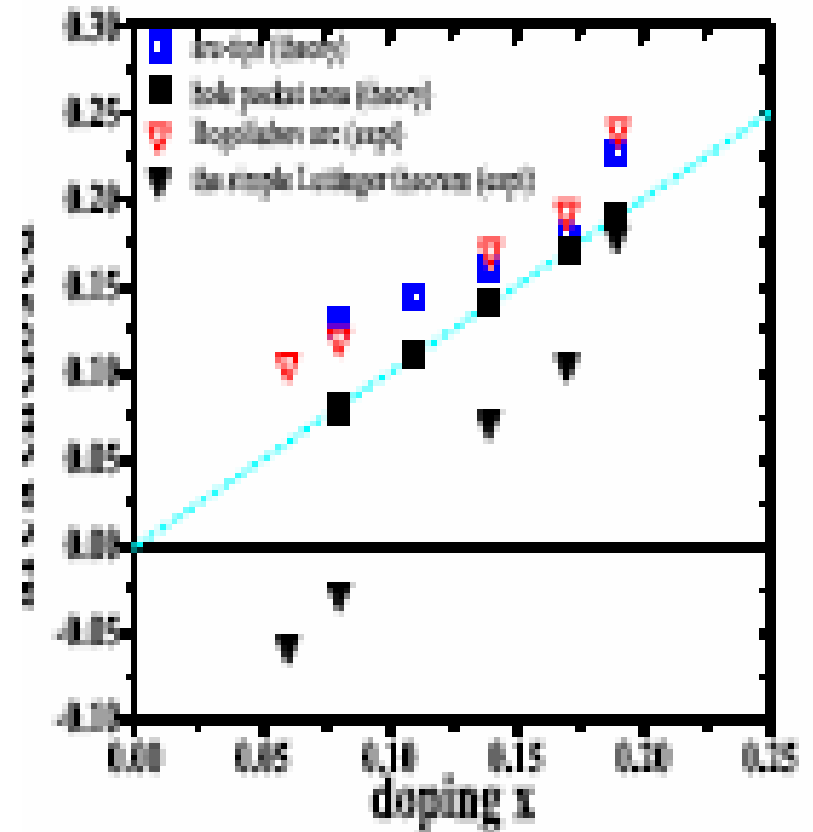


Fig. 3: (Color online) The red curves are the contours of the constant QP energy below and close to the Fermi energy. The black dots are the turning points deduced from STM interference data. The dashed blue lines are the hole Fermi pocket in the normal pseudogap state. The cyan curves are the turning points of the iso-energy contour of the corresponding band in the SC state. Note only the turning point of the iso-energy contour with the largest spectral weight are shown.



Fits to QP dispersion using YRZ ansatz for SC propagator

K.-Y. Yang et al EPL '09

Conclusions

- Increasing expt. evidence that the Fermi Surface is truncated to pockets by a RVB gap which opens on the umklapp surface in the underdoped region at $x < x_c$
- Superconductivity can be driven on the pockets by scattering of Cooper hole pairs into gapped regions
- Does not explain everything -
e.g. Quantum Oscillations at high B, Stripes, Magnetism etc.
- The YRZ ansatz is the simplest way to partially truncate the Fermi Surface but is it fully correct ?